MOLECULAR AND CELLULAR BIOLOGY, Sept. 2000, p. 6646–6658 Vol. 20, No. 18
0270-7306/00/$04.00+0

Meiotic Segregation, Synapsis, and Recombination Checkpoint Functions Require Physical Interaction between the Chromosomal Proteins Red1p and Hop1p

DANA WOLTERING,[1] BRIDGET BAUMGARTNER,[1] SANDIPAN BAGCHI,[1] BRITTANY LARKIN,[1] JOSEF LOIDL,[2] TERESA DE LOS SANTOS,[1] AND NANCY M. HOLLINGSWORTH[1]*

Department of Biochemistry and Cell Biology, Institute for Cell and Developmental Biology, State University of New York at Stony Brook, Stony Brook, New York 11794-5215,[1] and Department of Cytology and Genetics, Institute of Botany, University of Vienna, A-1030 Vienna, Austria[2]

Received 31 January 2000/Returned for modification 28 March 2000/Accepted 12 June 2000

In yeast, *HOP1* and *RED1* are required during meiosis for proper chromosome segregation and the consequent formation of viable spores. Mutations in either *HOP1* or *RED1* create unique as well as overlapping phenotypes, indicating that the two proteins act alone as well as in concert with each other. To understand which meiotic processes specifically require Red1p-Hop1p hetero-oligomers, a novel genetic screen was used to identify a single-point mutation of *RED1*, *red1-K348E*, that separates Hop1p binding from Red1p homo-oligomerization. The Red1-K348E protein is stable, phosphorylated in a manner equivalent to Red1p, and undergoes efficient homo-oligomerization; however, its ability to interact with Hop1p both by two-hybrid and coimmunoprecipitation assays is greatly reduced. Overexpression of *HOP1* specifically suppresses *red1-K348E*, supporting the idea that the only defect in the protein is a reduced affinity for Hop1p. *red1-K348E* mutants exhibit reduced levels of crossing over and spore viability and fail to undergo chromosome synapsis, thereby implicating a role for Red1p-Hop1p hetero-oligomers in these processes. Furthermore, *red1-K348E* suppresses the *sae2*/*com1* defects in meiotic progression and sporulation, indicating a previously unknown role for *HOP1* in the meiotic recombination checkpoint.

Sexual reproduction requires the formation of haploid gametes from diploid cells. This result is achieved by meiosis, a cell division in which two rounds of chromosome segregation follow a single round of chromosome duplication, thereby reducing the number of chromosomes in half in such a way that each gamete receives only a single copy of each homolog. Prophase of meiosis is comprised of a tightly coordinated series of events in which homologous chromosomes undergo pairing, recombination, and synapsis, culminating in the segregation of homologs to opposite poles at the first meiotic division (MI).

Genetic studies in a variety of organisms have shown that proper MI chromosome segregation requires that homologous chromosomes be physically connected by crossovers (5). Crossovers by themselves are insufficient to direct disjunction, however. Work in the budding yeast *Saccharomyces cerevisiae* indicates that for crossovers to be effective in segregation, they must occur in the context of a specific chromosomal structure, the synaptonemal complex (SC) (13, 36). The SC is formed when sister chromatids condense along a protein core to form axial elements (AEs). Homologous AEs are then connected by proteins that comprise the central region (15). Mutants that disrupt the central region have very modest effects on recombination and disjunction, although crossover interference is abolished (10, 44). In contrast, mutants that disrupt AE formation exhibit defects in sister chromatid cohesion, recombination, and chromosome segregation (4, 23, 36). Analysis of genes encoding AE components may therefore provide insight into the mechanisms by which crossovers work.

* Corresponding author. Mailing address: Department of Biochemistry and Cell Biology, SUNY Stony Brook, Stony Brook, NY 11794-5215. Phone: (631) 632-8581. Fax: (631) 632-8575. E-mail: nhollin@notes.cc.sunysb.edu.

In yeast, two meiosis-specific components of AEs essential for the production of viable spores are encoded by *HOP1* and *RED1* (18, 36, 43). Homologs of Hop1p exist in both *Arabidopsis* and *Caenorhabditis elegans* (20, 50). Mutation of the genes encoding these homologs creates meiotic mutant phenotypes (9, 50), indicating that *HOP1* function is conserved throughout evolution. Several lines of evidence suggest that *HOP1* and *RED1* work together. The two proteins colocalize to AEs and have been demonstrated to physically interact using two-hybrid and coimmunoprecipitation (co-IP) assays (11, 20, 43). In addition to low spore viability, *hop1* and *red1* mutants display a number of other phenotypes in common. For example, *HOP1* and *RED1* have been placed in the same genetic epistasis group for their effects on meiotic gene conversion (36). Mutations in both genes reduce, but do not eliminate, interhomolog recombination without affecting intrachromosomal recombination (17, 29, 36). The spore inviability of *red1* and *hop1* is rescued by *spo13*, a mutant that causes a single division meiosis, thereby removing the need for crossovers to segregate homologs (17, 36). Neither mutant can rescue a *rad52 spo13* diploid (29), however, presumably due to a failure in resolving aberrantly processed recombination events. Homolog pairing is reduced in spreads of chromosomes from *hop1* and *red1* diploids, and no SC is present (18, 33, 36).

The fact that Hop1p and Red1p interact and that the mutants have some common phenotypes suggests that Red1p-Hop1p complexes are required for some critical meiotic functions. However, because the phenotypes of the two mutants are not identical, both *HOP1* and *RED1* must function independently during meiosis as well. *RED1*, but not *HOP1*, is required for wild-type levels of sister chromatid cohesion (4). Whereas no chromosomal structures are seen in *red1* mutants (36), *hop1* mutants can form at least pieces of AEs (26). In isogenic strains, *red1* and *hop1* were observed to reduce interhomolog

recombination to different amounts, with *hop1* having the stronger defect (29, 36). Meiotic sister chromatid exchange is elevated in *red1*, but not *hop1*, mutants (45). In some strain backgrounds, *hop1* and *red1* mutants appear completely defective in the formation of double-strand breaks (DSBs) (29), while in the SK1 strain background, DSBs are reduced to a far greater extent in *hop1* than in *red1* strains (cited in reference 39; 49) (see below). Red1p is present on chromosomes during zygotene prior to Hop1p and remains on chromosomes during pachytene after Hop1p has left (43).

To distinguish meiotic processes that require Red1p-Hop1p hetero-oligomers from those that do not, we used a novel genetic screen to identify a mutation of *RED1* (*red1-K348E*) that specifically abolishes the ability of Red1p to interact with Hop1p. Phenotypic analysis of *red1-K348E* diploids revealed that Red1p-Hop1p complexes are essential in creating functional crossovers as well as for SC formation. Furthermore, this mutant enabled the discovery of a role for *HOP1* in the checkpoint that monitors the progression of recombination intermediates during meiosis.

MATERIALS AND METHODS

Plasmids. Plasmids for this study were constructed by standard procedures (28), using the *Escherichia coli* strains BSJ72 and XL1-Blue. A list of plasmids is given in Table 1. pNH223 was generated by cloning the 2.5-kb *Eco*RI/*Sal*I fragment from pNH207 into *Eco*RI/*Sal*I-digested pBTM116. The *lexA-red1-K348E* allele in pNH223-K348E was generated by site-directed mutagenesis (QuikChange kit from Stratagene) to introduce an A-to-G transition at position 1042 of *RED1* in pNH223. The presence of the mutation was confirmed by DNA sequencing. (All DNA sequencing was performed either by Research Genetics, Huntsville, Ala., or the Center for the Analysis and Synthesis of Macromolecules, State University of New York at Stony Brook.)

The *lexA-RED1*$_{1\text{-}426}$ plasmid (pDW28) was created by cloning the 1.2-kb *Eco*RI/*Bgl*II fragment from pNH207 into pSTT91 cut with *Eco*RI/*Bam*HI. Fusion to vector sequences results in the addition of eight amino acids (RSVDL QPS) to the C terminus of Red1p. pSB5 contains the *RED1*$_{1\text{–}426}$ fragment with the K348E mutation. This plasmid was constructed identically to pDW28 except that the 1.2-kb *Eco*RI/*Bgl*II fragment was obtained from pNH223-K348E. The truncation plasmids pDW35 (*lexA-RED*$_{1\text{–}326}$), pDW61 (*lexA-RED1*$_{1\text{–}359}$), and pDW62 (*lexA-RED1*$_{1\text{–}400}$) were all constructed by PCR using pNH207 as the template and Vent polymerase (New England Biolabs, Beverly, Mass.). Primers were designed to create at the 3′ end a *Bgl*II site which, when cloned into the *Bam*HI site of pSTT91, produces the same eight-amino-acid tail that is present in pDW28. The *RED1* portions of all three plasmids were sequenced to ensure that no mutations were introduced by PCR. The *lexA-RED1*$_{536\text{–}827}$ allele was also created by PCR. Primers were designed to put an *Eco*RI site at the 5′ end in frame with the *Eco*RI site in *lexA* in pSTT91. The 3′ primer introduces a *Bam*HI site downstream of the *RED1* stop codon. The PCR fragment was digested with *Eco*RI and *Bam*HI and ligated into pSTT91 to generate pDW58.

The *GAD* fusion to codons 330 to 426 of *RED1* (pDW54) was generated by PCR to amplify a fragment containing an *Eco*RI site upstream of position 330, a stop codon after position 426, and an *Xho*I site at the 3′ end. This fragment was digested with *Eco*RI and *Xho*I and ligated into pACTII (provided by J. Bailis, Yale University). For *GAD-red1-K348E*, the K348E mutation was introduced by site-directed mutagenesis into pJ63.

The *red1*Δ*::ADE2* deletion was generated by digesting pNH124 with *Cla*I and *Eco*RV and purifying the vector backbone. PCR was used to generate a fragment containing *ADE2* with *Cla*I and *Pvu*II at the ends. The PCR fragment was digested with *Cla*I and *Pvu*II and ligated into the pNH124 *Cla*I/*Eco*RV backbone to make pNH234. The *RED1 URA3* integrating plasmid pSB3 was constructed by subcloning the 3.3-kb *Hin*dIII fragment from pB64 into pRS306. This plasmid was then subjected to site-directed mutagenesis as described above, thereby making the *red1-K348E* mutation in pSB3-K348E. The *red1-K348E* allele was completely sequenced to ensure that no additional mutations were introduced by the mutagenesis. pBB14 and pBB16 were created by isolating *Not*I/*Sal*I fragments from pSB3-K348E and pSB3, respectively, and ligating them into *Not*I/*Sal*I-digested pRS402. For pBB19, a 3.2-kb *Bam*HI/*Nsi*I fragment from pMJ77 containing *ARG4* was cloned into *Bam*HI/*Nsi*I-digested pSB3-K348E. The *red1-K348E-3HA* allele in pNH212-K348E was created by site-directed mutagenesis of *RED1-3HA* in pNH212. Sequencing of the entire gene confirmed the absence of any additional mutations. The *HOP1 ADE2* overexpression plasmid, pDW72, was generated by cloning a 5.2-kb *Bgl*II fragment from pNH34 into *Bam*HI-cut pRS422.

Yeast strains and media. The genotypes of strains used in this work are listed in Table 2. Liquid and solid media have been described elsewhere (11, 47).

NH214 was constructed in several steps. First the *RED1* gene was deleted from two different haploid strains by transformation with a 3.5-kb *Pst*I fragment from pNH234. Each haploid was subsequently transformed with pSH18-34ΔSpe (provided by S. Hollenberg, Oregon Health Sciences University) digested with *Stu*I to target integration of the plasmid to *ura3*. This plasmid contains a *lexA*$_{op}$*-lacZ* reporter gene. The two haploids were then mated to create NH214. The NH246 series of diploids was generated by first deleting the *RED1* gene from BR1373-6D and 5787-21-4 using *red1*Δ*::ADE2*. Each haploid was then transformed with pRS306, pSB3, or pSB3-K348E digested with *Stu*I to target integration to the *ura3* locus. The appropriate transformants were mated to create NH246::pRS306, NH246::pSB3, and NH246::pSB3-K348E. To convert the NH246 diploids to Spo13$^+$, one haploid parent of NH246 containing either pRS306, pSB3, or pSB3-K348E was transformed with the *TRP1 SPO13* integrating plasmid, pNH20 (17). The resulting transformants were then crossed with the other parent carrying the appropriate *RED1* plasmid (or vector) to regenerate the diploids.

The SK1 diploids were generated using transformed derivatives of two different combinations of parental strains (S2683 × RKY1145 and NH212-1-1 × NH212-35-1 [Table 2]). NH212-1-1 and NH212-35-1 are haploid segregants from a cross between S2683ade2 and RYK1145red1. All of the SK1 diploids should, therefore, be isogenic with the exception of the markers listed in the genotypes. YTS3 and DW10 are isogenic diploids described in reference 11. YTS3::pRS306, YTS3::pSB3, and YTS3::pSB3-K348E were created by transforming the haploid parents with *Stu*I-digested pRS306, pSB3, and pSB3-K348E followed by mating to form the diploids. For NH311, the *ade2-Bgl* mutation was introduced into S2683hop1 and RKY1145hop1 as described previously (11). The *SAE2* gene was subsequently deleted using an *sae2*Δ*::URA3* fragment from pME1220 (generously supplied by J. Engebrecht, State University of New York at Stony Brook). Each haploid was transformed with pRS402 and then mated to form NH311. NH305 was generated by integrating either pRS402, pBB14 (*red1-K348E*), or pBB16 (*RED1*) cut with *Stu*I into the SK1 haploids NH212-1-1 and NH212-35-1

TABLE 1. Plasmids used

Name	Relevant genotype	Reference or source
pBTM116	2μm *lexA TRP1*	16
pSTT91	2μm *lexA TRP1 ADE2*	S. Tafrov
pNH207	2μm *lexA-RED1*$_{1\text{–}827}$ *TRP1 ADE2*	20
pNH223	2μm *lexA-RED1*$_{1\text{–}827}$ *TRP1*	This work
pB715	2 μm *lexA-red1-B715 TRP1*	This work
pNH223-K348E	2μm *lexA-red1-K348E TRP1*	This work
pDW35	2μm *lexA-RED1*$_{1\text{–}326}$ *TRP1 ADE2*	This work
pDW28	2μm *lexA-RED1*$_{1\text{–}426}$ *TRP1 ADE2*	This work
pSB5	2μm *lexA-red1*$_{1\text{–}426}$*-K348E TRP1 ADE2*	This work
pDW61	2μm *lexA-RED1*$_{1\text{–}359}$ *TRP1 ADE2*	This work
pDW62	2μm *lexA-RED1*$_{1\text{–}400}$ *TRP1 ADE2*	This work
pDW58	2μm *lexA-RED1*$_{536\text{–}827}$ *TRP1 ADE2*	This work
pLP27	2μm *lexA-HOP1 TRP1*	20
pACTII	2μm *GAD LEU2*	2
pNH108	2μm *GAD-HOP1 LEU2*	20
pJ63	2μm *GAD-RED1*$_{1\text{–}827}$ *LEU2*	4
pJ63-K384E	2μm *GAD-red1-K348E*$_{1\text{–}827}$ *LEU2*	This work
pGAD-RED1$_{537\text{–}827}$	2μm *GAD-RED1*$_{537\text{–}827}$ *LEU2*	46
pDW54	2μm *GAD-RED1*$_{330\text{–}426}$ *LEU2*	This work
pNH124	*RED1*	20
pNH234	*red1*Δ*::ADE2*	This work
pB64	*RED1 URA3 CEN ARS*	37
pRS306	*URA3*	41
pSB3	*RED1 URA3*	This work
pSB3-K348E	*red1-K348E URA3*	This work
pRS402	*ADE2*	7
pBB16	*RED1 ADE2*	This work
pBB14	*red1-K348E ADE2*	This work
pMJ77	*ARG4*	M. Lichten
pBB19	*red1-K348E ARG4*	This work
p1b-1	2μm *RED1 URA3*	19
pNH212	2μm *RED1-3HA URA3*	11
pNH212-K348E	2μm *red1-K348E-3HA URA3*	This work
pSH18-34ΔSpe1	*lexA*$_{op}$*-lacZ* 2μm *URA3*	S. Hollenberg
pNH20	*SPO13 TRP1*	17
pME1220	*sae2::URA3*	J. Engebrecht
YEp24	2μm *URA3*	34
pNH83	2μm *HOP1 URA3*	19
pRS422	2μm *ADE2*	7
pNH34	*HOP1*	17
pDW72	2μm *HOP1 ADE2*	This work
pME1210	0.9-kb chromosome III fragment in SK$^+$	J. Engebrecht

TABLE 2. *S. cerevisiae* strains used

Strain	Genotype	Source or reference
L40	*MAT***a** *his3Δ200 trp1-90 leu2-3,112 ade2 lys2::lexA HIS3 LYS2 gal80 ura3::lexA lacZ URA3*	R. Sternglanz
NH214	*MAT***a** *leu2 ura3::*pSH18-34ΔSpe *(lexA$_{op}$-lacZ URA3) CAN1 trp1 his3 ade2 red1Δ::ADE2 LYS1 CYH2 tyr1* / *MATα leu2 ura3::*pSH18-34ΔSpe *(lexA$_{op}$-lacZ URA3) can1 trp1 his3 ade2 red1Δ::ADE2 lys1 cyh2 TYR1*	This work
BR1373-6D	*MAT***a** *leu2-27 his4-280 ura3-1 ade2-1 thr1-1 trp1-1 spo13::ura3-1 lys2 arg4-8 cyh10*	J. Engebrecht
5787-21-4	*MATα cdc10-2 trp1 ura3 can1 cyh2 spo13-1 ade2-1*	17
NH246	*MAT***a** *CDC10 leu2 his4 arg4-8 thr1-1 ura3-1 CAN1 trp1-1 cyh10 ade2-1 spo13::ura3-1 CYH2 red1Δ::ADE2* / *MATα cdc10 LEU2 HIS4 ARG4 THR1 ura3 can1 trp1 CYH10 ade2-1 spo13-1 cyh2 red1Δ::ADE2*	This work
NH246::pRS306	Same as NH246 except *ura3::*pRS306 *(URA3)* / *ura3::*pRS306 *(URA3)*	This work
NH246::pSB3	Same as NH246 except *ura3::*pSB3 *(RED1 URA3)* / *ura3::*pSB3 *(RED1 URA3)*	This work
NH246::pSB3-K348E	Same as NH246 except *ura3::*pSB3-K348E *(red1-K348E URA3)* / *ura3::*pSB3-K348E *(red1-K348E URA3)*	This work
NH246::pRS306 Spo13$^+$	Same as NH246::pRS306 except *spo13::*pNH20 *(TRP1 SPO13)* / *spo13*	This work
NH246::pSB3 Spo13$^+$	Same as NH246::pSB3 except *spo13::*pNH20 *(TRP1 SPO13)* / *spo13*	This work
NH246::pSB3-K348E Spo13$^+$	Same as NH246::pSB3-K348E except *spo13::*pNH20 *(TRP1 SPO13)* / *spo13*	This work
RKY1145	*MAT***a** *leu2ΔhisG his4-x ura3 lys2 hoΔ::LYS2*	G. S. Roeder
S2683	*MATα leu2-K arg4-Nsp ura3 lys2 hoΔ::LYS2*	G. S. Roeder
YTS3[a]	*MAT***a** *leu2ΔhisG his4-x ARG4 ura3 lys2 hoΔ::LYS2 red1::LEU2* / *MATα leu2-K HIS4 arg4-Nsp ura3 lys2 hoΔ::LYS2 red1::LEU2*	11
YTS3::pRS306[a]	Same as YTS3 except *ura3::*pRS306 *(URA3)* / *ura3::*pRS306 *(URA3)*	This work
YTS3::pSB3[a]	Same as YTS3 except *ura3::*pSB3 *(RED1 URA3)* / *ura3::*pSB3 *(RED1 URA3)*	This work
YTS3::pSB3-K348E[a]	Same as YTS3 except *ura3::*pSB3-K348E *(red1-K348E URA3)* / *ura3::*pSB3-K348E (*red1-K348E URA3)*	This work
DW10[a]	*MAT***a** *leu2ΔhisG his4-x ARG4 ura3 lys2 hoΔ::LYS2 hop1::LEU2* / *MATα leu2-K HIS4 arg4-Nsp ura3 lys2 hoΔ::LYS2 hop1::LEU2*	11
NH311::pRS402[a]	*MAT***a** *leu2ΔhisG his4-x ARG4 ura3 lys2 hoΔ::LYS2 hop1::LEU2 ade2-Bgl::*pRS402 *(ADE2) sae2Δ::URA3* / *MATα leu2-K HIS4 arg4-Nsp ura3 lys2 hoΔ::LYS2 hop1::LEU2 ade2-Bgl::*pRS402 *(ADE2) sae2Δ::URA3*	This work
NH212-1-1	*MAT***a** *leu2 his4 ura3 lys2 hoΔLYS2 ade2-Bgl red1::LEU2*	This work
NH212-35-1	*MATα leu2-k ura3 lys2 hoΔLYS2 arg4-Nsp ade2-Bgl red1::LEU2*	This work
NH305[b]	*MAT***a** *leu2 his4 ura3 lys2 hoΔLYS2 ARG4 ade2-Bgl red1::LEU2* / *MATα leu2-k HIS4 ura3 lys2 hoΔLYS2 arg4-Nsp ade2-Bgl red1::LEU2*	This work
NH305::pRS402[b]	Same as NH305 except *ade2-Bgl::*pRS402 *(ADE2)* / *ade2-Bgl*	This work
NH305::pBB16[b]	Same as NH305 except *ade2-Bgl::*pBB16 *(RED1 ADE2)* / *ade2-Bgl::*pBB16 *(RED1 ADE2)*	This work
NH305::pBB14[b]	Same as NH305 except *ade2-Bgl::*pBB14 *(red1-K348E ADE2)* / *ade2-Bgl::*pBB14 *(red1-K348E ADE2)*	This work
NH306[b]	Same as NH305 except *sae2Δ::URA3* / *sae2Δ-URA3*	This work
NH306::pRS402[b]	Same as NH306 except *ade2-Bgl::*pRS402 *(ADE2)* / *ade2-Bgl::*pRS402 *(ADE2)*	This work
NH306::pBB16[b]	Same as NH306 except *ade2-Bgl::*pBB16 *(RED1 ADE2)* / *ade2-Bgl::*pBB16 *(RED1 ADE2)*	This work
NH306::pBB14[b]	Same as NH306 except *ade2-Bgl::*pBB14 *(red1-K348E ADE2)* / *ade2-Bgl::*pBB14 *(red1-K348E ADE2)*	This work
NH306::pBB19	Same as NH306 except *ARG4* / *arg4::*pBB19 *(red1-K348E ARG4)*	This work

[a] SK1 diploid generated by crossing RYK1145 and S2683 transformed derivatives.
[b] SK1 diploid generated by crossing 212-1-1 and 212-35-1 derivatives. 212-1-1 and 212-35-1 are haploid segregants from a cross of transformed derivatives of the SK1 haploids RYK1145 and S2683.

and then mating to form the diploids NH305::pRS402, NH305::pBB14, and NH305::pBB16. To create the *red1::LEU2 sae2*Δ diploid, NH306, the *SAE2* gene was first deleted in the SK1 haploids NH212-1-1 and NH212-35-1 by transformation with an *sae2Δ::URA3* fragment from pME1220. Plasmids pRS402, pBB14, and pBB16 were digested with *Stu*I and integrated at *ade2* in the two *red1::LEU2 sae2*Δ haploids. Mating of the appropriate transformants produced NH306::pRS402, NH306::pBB14, and NH306::pBB16. For NH306::pBB19, pBB19 was linearized with *Nhe*I to target integration to *ARG4* and transformed into NH212-35-1sae2Δ The resulting transformant was then mated to NH212-1-1sae2Δ to make the diploid. All disruptions and/or deletions were confirmed by Southern blot analysis (data not shown).

***RED1* separation-of-function mutant screen.** To assay putative *lexA-red1* mutants for both complementation of the *red1* spore inviability phenotype and the two-hybrid interaction with *GAD-RED1*$_{537–827}$, we used yeast strain NH214.

NH214 is diploid, homozygous for *red1*Δ, and heterozygous for two drug resistance markers, *can1* and *cyh2*. Because *can1* and *cyh2* are recessive, the diploid is sensitive to the drugs canavanine and cycloheximide. The haploidization that occurs during meiosis results in one-fourth of the spores being resistant to both drugs. Spore viability can therefore be easily assessed qualitatively by plate assays on medium lacking arginine and containing canavanine and cycloheximide (−Arg + Can + Cyh). In addition, NH214 is homozygous for a *lexA*$_{op}$*-lacZ* reporter construct, thereby enabling detection of two-hybrid interactions. NH214 containing plasmid pGAD-RED1$_{537–827}$ was transformed with a *lexA-RED1* plasmid (pNH223) that was gapped with *Bgl*II to delete the 5′ half of *RED1* encoding amino acids 1 to 426 along with a library of PCR fragments spanning the gapped region. This library was generated using primers complementary to sequences 200 bp upstream of the 5′ *Bgl*II site and 200 bp downstream of the 3′ *Bgl*II site in pNH223 with pNH223 as the template. *Taq* polymerase (Gibco-BRL, Gaithersburg, Md.) and standard reaction conditions were used for the PCR (0.2 mM deoxynucleoside triphosphates, 1.5 mM $MgCl_2$, 1 μM each primer). The intrinsic error rate of *Taq* is high enough that amplification of the 1.5-kb fragment resulted in ~10% null alleles of *RED1*. Transformants result when recombination between the PCR fragments and the gapped pNH223 generates intact plasmids (31). Transformants were patched onto −Trp, −Leu selective medium, replica plated to sporulation plates at 30°C to induce the cells to undergo meiosis, and then plated to −Arg + Can + Cyh to assay for complementation. Plasmids that failed to complement were then tested for the ability to interact with *GAD-RED1*$_{537–827}$ using filter assays to detect the production of β-galactosidase. Those plasmids that still interacted with *GAD-RED1*$_{537–827}$ were further analyzed.

Out of 13,234 transformants, 12.6% failed to complement the spore viability defect. Of these, 3.1% were likely due to vector religation, giving a frequency of *red1* mutant alleles of 9.5%. One of these plasmids, pB715, gave reduced growth after sporulation on −Arg + Can + Cyh plates but continued to produce a strong positive signal with *GAD-RED1*$_{537–827}$ by filter assays. This plasmid was recovered from yeast and introduced into *E. coli*. pB715 was then transformed into the two-hybrid reporter strain L40 for quantitative liquid β-galactosidase assays and into a *red1* diploid for tetrad dissection.

Co-IP experiments and immunoblot analysis. Hop1p, Red1-3HAp (Red1p tagged with three copies of the hemagglutinin epitope [HA]), and Red1-K348E-3HAp were immunoprecipitated from meiotic extracts as described previously (11). The proteins were visualized by immunoblot analysis using an ECL kit from Amersham Pharmacia Biotech and anti-Hop1p (α-Hop1p) (11) or α-HA antibodies (BAbCo).

β-Galactosidase assays. β-Galactosidase filter assays were performed as described elsewhere (20). Liquid β-galactosidase assays were performed as described in reference 14.

Cytology. For electron microscopy, cells were sporulated for 4.5 h, and chromosome spreads were prepared and analyzed as described by Loidl et al. (25).

For meiotic time courses, cultures from three independent colonies of each strain were sporulated as described previously (11). Cells were removed at different time points and fixed with 3.7% formaldehyde for 24 h. The cells were then washed twice with phosphate-buffered saline and stained with 1 μM DAPI (4′,6-diamidino-2-phenylindole) for 10 min. After washing, the cells were sonicated and mounted onto lysine-coated slides for fluorescence microscopy. Two hundred cells were counted for each culture. Binucleate cells were counted as having completed MI, while tetranucleate cells were counted as having completed MII. Sporulation was assessed by light microscopy.

DSB assays. Cells were sporulated as described previously (11). DNA was isolated in plugs as described by Borde et al. (6). The DNA was digested in the plugs by using a slight modification of the protocol provided by T. Wu, V. Borde, and M. Lichten (personal communication). One-half of each plug (~35 μl) was soaked with gentle mixing twice for 30 min, first in 5 ml of Tris-EDTA (pH 8.0) and then in 5 ml of 1× NEB buffer 3 (New England Biolabs). The plugs were transferred to 1.5-ml microcentrifuge tubes, and the agarose was melted at 65°C for 10 min. After equilibration at 37°C for 5 min, 20 U of *Bgl*II was added and incubation was continued for 2 h at 37°C. An additional 10 U of *Bgl*II was added; the tubes were chilled on ice for 15 min and then incubated at 37°C overnight. To load the gel, the digests were heated at 65°C for 5 min and loaded onto a "dry" (i.e., not submerged in buffer) 0.75% Tris-borate-EDTA agarose gel. After 3 min, the gel was immersed in buffer and run for 24 h at 20 V. The gel was prepared for hybridization and probed as described elsewhere (30). A ^{32}P-labeled 0.9-kb *Hin*dIII fragment that detects the *THR4* DSB hot spot (48) from pME1210 was used as a probe. Quantitation of the DSB fragments was performed using a Molecular Dynamics PhosphorImager and ImageQuant 1.11 software. To account for different amounts of DNA loaded, DSB fragments were normalized to the appropriate parental bands.

RESULTS

Deletion analysis of *RED1* indicates that Red1p homo-oligomerization occurs using the C-terminal 291 amino acids. Previous work had demonstrated that full-length *lexA-RED1*$_{1–827}$ interacts with a C-terminal fragment of Red1p containing amino acids 537 to 827 (20). This result suggested that Red1p is capable of homo-oligomerization through its carboxy terminus. Consistent with this hypothesis, *GAD-RED1*$_{537–827}$ does not interact with several different C-terminal truncations of *RED1* (Fig. 1). To test whether the C-terminal 291 amino acids are sufficient for Red1p-Red1p interaction, a *lexA* fusion to codons 536 to 827 of *RED1* was assayed for interaction with *GAD-RED1*$_{537–827}$. A strong positive signal was obtained with this combination (Fig. 1), indicating that Red1p homo-oligomerization is mediated by the C-terminal part of the protein.

Secondary structure programs predict two distinct regions of α helix in Red1p. One region is located near the middle of Red1p, between amino acids 360 and 400; the other is near the end of the protein, between amino acids 760 and 800 (Fig. 1). It is possible that Red1p may interact with itself through these α-helical regions, one of which is contained within the C-terminal fragment known to undergo homo-oligomerization. To see whether the internal region of putative α helix can promote Red1p-Red1p interaction, a fragment of *RED1* encoding amino acids 330 to 426 was fused to *GAD* and tested for its interaction with full-length *lexA-RED1* as well as two Red1p C-terminal truncations. No signal was observed with any of these combinations, indicating that homo-oligomerization is specific to the C-terminal fragment of *RED1* (Fig. 1).

Deletion analysis of *RED1* reveals a 30-amino-acid domain that mediates interaction with *HOP1*. Previous work from our lab demonstrated a two-hybrid interaction between the C-terminal 291 amino acids of Red1p and Hop1p (20). In the course of this work we discovered that *GAD-HOP1* produces a much stronger signal when combined with the *lexA-RED1*$_{1–426}$ C-terminal truncation (Fig. 2). Deletion of an additional 100 amino acids from the 426-amino-acid amino-terminal fragment (*lexA-RED1*$_{1–326}$) abolishes the *GAD-HOP1* interaction (Fig. 2). The failure to see an interaction with *lexA-RED1*$_{1–326}$ is not because the protein is unstable, as LexA-RED1$_{1–326}$p was readily detectable by Western blot analysis using α-LexA antibodies (data not shown). These experiments suggested that a Hop1p interaction domain is contained within the 100 amino acids located between positions 326 and 426. To determine whether this region is sufficient for Hop1p interaction, an internal fragment of *RED1* containing codons 330 to 426 was tested for interaction with *HOP1*. Because this fragment activated transcription of the *lacZ* reporter when fused to *lexA*, the fusion was made to *GAD* and assayed in combination with *lexA-HOP1*. The strong positive signal observed for these two proteins indicates that a Hop1p interaction domain is contained within these 97 amino acids of Red1p (Fig. 2). The fact that this region of *RED1* contains the region of internal putative α helix suggested the possibility that the α helix may mediate complex formation with Hop1p. This hypothesis was tested using two additional C-terminal truncations of *RED1*. The *lexA-RED1*$_{1–400}$ protein ends just after the predicted α-helical domain, while the *lexA-RED1*$_{1–359}$ protein deletes the predicted α helix. Since *lexA-RED1*$_{1–359}$ still interacts with *GAD-HOP1* (Fig. 2), the putative α-helical domain is not required for Hop1p interaction. Comparison of the endpoints of the various *RED1* deletion plasmids maps this Hop1p interaction domain of Red1p to the 30 amino acids located between residues 330 and 359.

A novel screen for *RED1* separation-of-function mutants identifies a single amino acid that is essential for Red1p-Hop1p interaction. To identify mutations of *RED1* defective in functions other than homo-oligomerization, we used a novel strategy that combines PCR mutagenesis, complementation analysis, and two-hybrid assays. *lexA-RED1* was mutagenized using PCR, and the resulting transformants were screened for

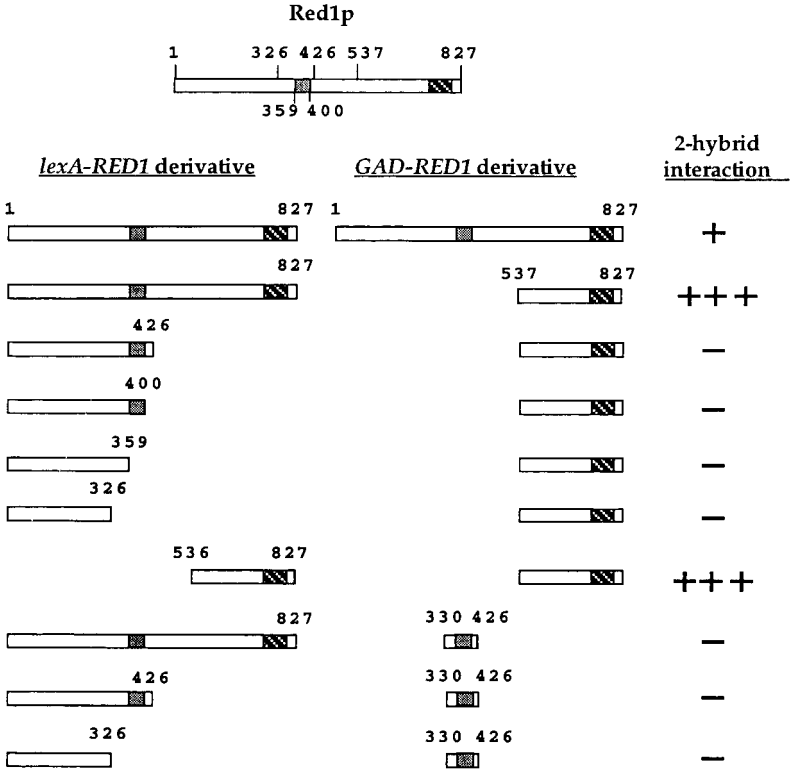

FIG. 1. Two-hybrid analysis of various *RED1* constructs. The two boxes present in Red1p represent regions of predicted coiled-coil structure. Protein-protein interactions were assayed by β-galactosidase filter assays in strain L40. Plasmids used: pNH223 (*lexA-RED1*$_{1–827}$); pDW35 (*lexA-RED1*$_{1-326}$); pDW61 (*lexA-RED1*$_{1–359}$); pDW62 (*lexA-RED1*$_{1-400}$); pDW28 (*lexA-RED1*$_{1–426}$); pDW58 (*lexA-RED1*$_{536–827}$); pJ63 (*GAD-RED1*$_{1–827}$); pGAD-RED1$_{537–827}$ and pDW54 (GAD-RED1$_{330–426}$). One plus sign indicates that the cells turned blue in 90 min at 30°C; three plus signs indicates the cells turned blue by 15 min; a minus sign indicates a failure to turn blue by 4 h.

a failure to complement the *red1* spore inviability phenotype while retaining the ability to interact with *GAD-RED1*$_{527–837}$ (see Material and Methods). Since Red1p homo-oligomerization occurs through the C-terminal part of the protein, requiring the mutant protein to interact with Gad-Red1$_{537–827}$p should eliminate mutant alleles that result from stop codons that truncate the protein. Because deletion analysis indicated that a Hop1p interaction domain is contained within the amino-terminal half of Red1p, mutagenesis was targeted to the part of *RED1* that encodes amino acids 1 to 426.

One allele of *RED1*, *lexA-red1-B715* that was obtained exhibited reduced spore viability in a *red1* diploid but still interacted at wild-type levels with *GAD-RED1*$_{537–827}$ (data not shown). To determine the nature of the mutation responsible for the *red1-B715* mutant phenotypes, the 5′ half of the *lexA-red1-B715* allele was sequenced and compared to the *RED1* gene in pNH223. Three nucleotide changes were found: an A-to-G transition that creates a silent mutation in amino acid 310 (R to R); an A-to-G transition which changes a lysine to glutamic acid (K to E) at amino acid 348; and a T-to-C transition which changes a serine to proline at amino acid 404 (S to P). Only one of these mutations, K348E, falls into the 30-amino-acid domain established by deletion analysis to be necessary for Hop1p interaction. Site-directed mutagenesis was used to introduce the K348E mutation into the *lexA-RED1* gene, thereby creating the *lexA-red1-K348E* allele in pNH223-K348E.

The *lexA-red1-K348E* allele is phenotypically identical to *lexA-red1-B715*. When pNH223-K348E was transformed into a *red1* diploid and assayed for spore viability, only 3.9% viable spores (112 asci) were observed, compared to 68.5% viable spores (138 asci) exhibited by *lexA-RED1* (pNH223) and 1.6% viable spores (92 asci) for *lexA* (pBTM116). Homo-oligomerization was assayed in two different ways. First, *lexA-red1-K348E* was tested with *GAD-RED1*$_{537–827}$, the combination used in the mutant screen, and the interaction observed with the K348E mutant was equivalent to that for *lexA-RED1* (Table 3). Even higher than wild-type levels of β-galactosidase were produced when the mutation was homozygous (*lexA-red1-K348E*/*GAD-red1-K348E*), indicating that homo-oligomerization in the context of the full-length protein is unaffected by the K348E mutation as well (Table 3).

The failure of *lexA-red1-K348E* to complement indicates that some essential meiotic function is affected in the mutant that is independent of Red1p homo-oligomerization. A candidate for this essential function is the ability of Red1p to interact with Hop1p. This idea is supported by the finding that *lexA-red1-K348E* does not interact with *GAD-HOP1* in the two-hybrid system (Table 3). Because the signal for Red1p-Hop1p interaction in the two-hybrid system is fairly weak (~0.5 U of β-galactosidase activity) when full-length *lexA-RED1* is used, the K348E mutation was tested for the *GAD-HOP1* interaction in the context of the *lexA-RED1*$_{1–426}$ truncation. The *lexA-RED1*$_{1–426}$ plasmid produces nearly 50 U of β-galactosidase activity in combination with *GAD-HOP1*, thereby providing a much higher signal-to-noise ratio. No interaction is observed with *GAD-HOP1*, however, when this *lexA-RED1* truncation contains the K348E mutation (Table 3). These results clearly define the lysine at position 348 as a critical residue for *RED1*

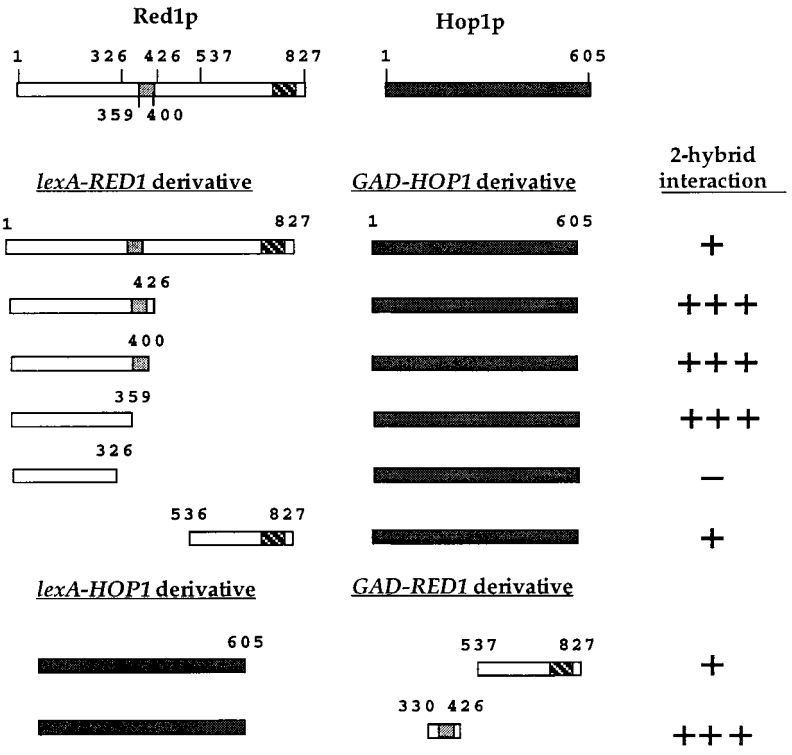

FIG. 2. Two-hybrid analysis of various *RED1* constructs with *HOP1*. Protein-protein interactions were assayed in L40 by β-galactosidase filter assays in strain L40. Plasmids used: pNH223 (*lexA-RED1*$_{1–827}$); pDW35 (*lexA-RED1*$_{1–326}$); pDW61 (*lexA-RED1*$_{1–359}$); pDW62 (*lexA-RED1*$_{1–400}$); pDW28 (*lexA-RED1*$_{1–426}$); pDW58 (*lexA-RED1*$_{536–827}$); pLP27 (*lexA-HOP1*); pJ63 (*GAD-RED1*$_{1–827}$); pGAD-RED1$_{537–827}$; pDW54 (*GAD-RED1*$_{330–426}$) and pNH108 (*GAD-HOP1*). One plus sign indicates that the cells turned blue in 90 min at 30°C; three plus signs indicates the cells turned blue by 15 min; a minus sign indicates a failure to turn blue by 4 h.

function, presumably due to its role in the binding of Red1p to Hop1p.

***Red1-K348E-3HAp* fails to interact with Hop1p in meiotic cells.** To test whether the Red1p-Hop1p interaction is disrupted when the proteins are in meiotic cells, co-IP experiments were performed. We have previously shown that Hop1p can coimmunoprecipitate an epitope-tagged version of Red1p called Red1-3HAp (11). Plasmids bearing an untagged allele of *RED1* (p1b-1), *RED1-3HA* (pNH212), and *red1-K348E-3HA* (pNH212-K348E) were transformed into the SK1 *red1* diploid, YTS3. The cells were transferred to sporulation medium for 3 h to induce meiosis, and extracts from the same number of cells were made for each strain. α-Hop1p or α-HA antibody was added to the extracts to immunoprecipitate Hop1p or Red1-3HAp, respectively. The amount of Red1-K348E-3HAp present in the IP is at least as much as the amount of Red1-3HAp (Fig. 3B), indicating that the mutant protein is stable. Red1p is known to be a *MEK1*-dependent phosphoprotein (4, 11). Red1-K348E-3HAp exhibits both phosphorylated and un-

TABLE 3. Quantitation of two-hybrid interactions

Plasmids[a]	Genotype		β-Galactosidase activity (Miller units)	*n*
	lexA-	*GAD-*		
pNH223/pGAD424	*RED1*		0.1 ± 0.0	32
pNH223-K384E/pACTII	*RED1*		0.1 ± 0.0	8
pNH223/pGAD-RED1$_{537–827}$	*RED1*	*RED1*$_{537–827}$	8.6 ± 1.7	16
pNH223-K348E/pGAD-RED1$_{537–827}$	*red1-K348E*	*RED1*$_{537–827}$	10.2 ± 1.1	8
pNH223/pJ63	*RED1*	*RED1*	1.2 ± 0.4	8
pNH223-K348E/pJ63-K348E	*red1-K348E*	*red1-K348E*	6.9 ± 0.1	8
pNH223/pNH108	*RED1*	*HOP1*	0.5 ± 0.0	16
pNH223-K348E/pNH108	*red1-K348E*	*HOP1*	0.0 ± 0.0	8
pDW28/pNH108	*RED1*$_{1–426}$	*HOP1*	49.5 ± 10.4	6
pSB5/pNH108	*red1*$_{1–426}$*-K348E*	*HOP1*	0.1 ± 0.0	8

[a] Plasmids were transformed into L40. Liquid β-galactosidase assays were performed as described in Materials and Methods. Units are expressed as mean plus and minus standard deviation. For the pNH223 controls, the data from several experiments performed on different days were pooled.

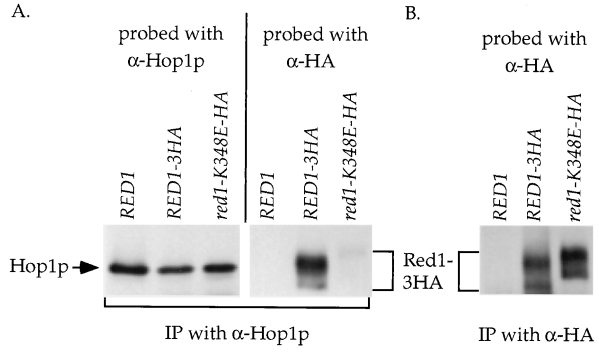

FIG. 3. Co-IP of different Red1-3HA proteins with Hop1p from meiotic extracts of SK1 diploids. Cells from YTS3 transformed with either p1b-1 (*RED1*), pNH212 (*RED1-3HA*), or pNH212-K348E (*red1-K348E-3HA*) were sporulated for 3 h. Hop1p and Red1-3HAp were immunoprecipitated from soluble extracts prepared from equivalent numbers of cells using α-Hop1p (A) or α-HA (B) antibody. The Hop1p IPs were first probed with α-HA to detect Red1-3HAp. The blot was then stripped and reprobed with α-Hop1p antibodies to detect Hop1p. The α-HA IPs were probed with α-HA antibodies.

TABLE 4. Spore viabilities for various alleles of *RED1* in the SK1 background

Strain/plasmid	Relevant genotype	% Spore viability (no. of asci)
Expt A[a]		
NH305::pBB16	*RED1*	100.0 (27)
NH305::pRS402	*red1::LEU2*	<1.0 (27)
NH305::pBB14	*red1-K348E*	<1.0 (27)
Expt B[b]		
NH305::pRS402/YEp24	*red1::LEU2*/2μm	<1.0 (26)
NH305::pRS402/pNH83	*red1::LEU2*/2μm *HOP1*	0.8 (60)
NH305::pBB14/YEp24	*red1-K348E*/2μm	3.0 (117)
NH305::pBB14/pNH83	*red1-K348E*/2μm *HOP1*	24.5 (202)

[a] Complementation of *red1::LEU2* by integrated alleles of *RED1*.
[b] Suppression of *red1-K384E* by overexpression of *HOP1*.

phosphorylated species of Red1p (Fig. 3B), demonstrating that the mutation does not disrupt the interaction of Red1p with kinases such as Mek1p. Red1-K348E-3HAp reproducibly runs at a slower mobility than Red1-3HAp. The reason for this is not clear, although the change in charge from lysine to glutamic acid may be involved. Similar levels of Hop1p are precipitated from all of the strains (Fig. 3A). Probing of the Hop1p IPs with α-HA antibodies reproduced the Red1-3HAp co-IP observed previously (Fig. 3A) (11). In contrast, very little Red1-K348E-3HA protein was found to coimmunoprecipitate with Hop1p. The two-hybrid experiments demonstrating a reduction in the ability of the Red1-K348Ep to interact with Hop1p have therefore been independently confirmed in meiotic cells.

The spore inviability phenotype observed for the *lexA-red1-K348E* mutant is due neither to *lexA* nor to misexpression of the protein. The mutation in *lexA-red1-K348E* is present in an artificial context: the *red1-K348E* gene is fused to *lexA* and is constitutively overexpressed on a high-copy-number plasmid. To determine whether any of these features contributed to the *red1-K348E* mutant phenotype, the K348E mutation was introduced by site-directed mutagenesis into *RED1* and cloned into an integrating plasmid (pBB14). Both *RED1* and *red1-K348E* were then integrated into the SK1 *red1* diploid NH305, and *RED1* function was assessed by measuring spore viability. In this strain background, the *red1-K348E* mutant produces very few viable spores (Table 4, experiment A), indicating that it is the point mutation that is solely responsible for the defect in spore viability.

The spore inviability of *red1-K348E* can be suppressed by overexpression of *HOP1*. If reduced affinity for Hop1p is the sole defect of the Red1-K348Ep, then overexpression of *HOP1* should suppress the *red1-K348E* spore inviability phenotype. The *HOP1* gene was overexpressed by placing it in a 2μm plasmid (pNH83) and introducing it into the SK1 NH305::pBB14 diploid. The resulting transformants were assayed for the production of viable spores by tetrad dissection. Overexpression of *HOP1* significantly increased spore viability in the *red1-K348E* strain (χ^2; $P < 0.001$), while the YEp24 vector had no effect (Table 4, experiment B). This suppression is specific to the *red1-K348E* mutant; the same low spore viability was observed in the *red1* null diploid both with and without excess *HOP1* (Table 4, experiment B). These experiments strongly argue that the formation of Red1p-Hop1p complexes is essential for the production of viable spores and support the idea that the only defect of Red1-K348Ep is its inability to efficiently interact with Hop1p.

The *red1-K348E* mutant exhibits an increased number of interhomolog crossovers compared to a *red1*Δ, but these crossovers are not effective in promoting proper meiotic chromosome segregation. To determine whether the *red1-K348E* mutant has any effect on crossing over between homologs, recombination was monitored in a diploid homozygous for *spo13* so that viable spores could be analyzed. *spo13* mutants undergo a single meiotic division, thereby obviating the need for crossovers to produce viable spores (27). The *red1*Δ *spo13* diploid, NH246, was transformed with either vector alone (pRS306), *RED1* (pSB3), or *red1-K348E* (pSB3-K348E). This diploid is a hybrid between the slow-sporulating BR and A346a strain backgrounds. The transformants were sporulated, and the resulting dyads were dissected. Both the *red1-K348E* and *red1*Δ mutants exhibited elevated levels of spore viability (73.5% [481 dyads] and 75.3% [504 dyads], respectively) relative to *RED1* (58.9% [698 dyads])—a phenomenon previously observed for a number of recombination-defective mutants (e.g., reference 10). The spore colonies were patched to YPAD and then replica plated to appropriate media to score heterozygous markers present on chromosomes III and VIII.

Consistent with published work from other labs, deletion of *RED1* reduced, but did not abolish, crossing over (Table 5). The *red1-K348E* mutant also reduced the number of crossovers compared to *RED1*, indicating that Red1p-Hop1p complexes are required for wild-type levels of interhomolog recombination (Table 5).

The *red1-K348E* mutant exhibited only a 2-fold reduction in crossing over, compared to the 11-fold decrease in the *red1*Δ mutant. One explanation for this difference would be that the *red1-K348E* allele was simply leaky. Given the existence of several mutants (e.g., *msh4*, *msh5*, *zip1*, and *zip2*) that exhibit a two- to threefold reduction in crossing over along with only a twofold reduction (to ~50%) in spore viability (8, 10, 21, 38, 44), the "leaky allele" hypothesis would predict that spore viability in the isogenic *red1-K348E SPO13* diploid should be approximately 50% as well. To determine whether the *red1-*

TABLE 5. Effect on meiotic interhomolog crossing over of *red1*Δ and *red1-K348E* mutants

NH246::	Relevant genotype	Map distance (centimorgans)[a]				Mean fold reduction
		HIS4-LEU2	*LEU2-CDC10*	*CDC10-MAT*	*ARG4-THR1*	
pSB3	*RED1*/*RED1*	18.3 (254)	13.1 (245)	22.2 (248)	12.1 (286)	1.0
pRS306	*red1*Δ[b]/*red1*Δ	0.7 (284)	1.6 (286)	1.7 (295)	2.0 (318)	10.9
pSB3-K348E	*red1-K348E*[b]/*red1-K348E*	4.7 (223)	7.8 (223)	9.8 (224)	6.2 (256)	2.3

[a] Calculated as described by Hollingsworth et al. (21).
[b] All values are statistically significantly different from the *RED1* values to the $P < 0.001$ level by χ^2 analysis.

TABLE 6. SC formation in various wild-type and mutant SK1 diploids[a]

Relevant genotype	Empty nuclei	Thin linear structures (AEs)	Short thick structures[b]	Long thick structures[b]	Zygotene SCs	Pachytene SCs
RED1	49	15	18	30	30	88
red1::LEU2	165	20	14	1	0	0
red1-K348E	123	21	36	21	0	0
hop1::LEU2	108	86	6	0	0	0

[a] YTS3 transformed with vectors pSB3 (*RED1*) and pSB3-K348E (*red1-K348E*), as well as DW10 (*hop1::LEU2*), were induced to undergo meiosis, and chromosome spreads were prepared for electron microscopy as described in Materials and Methods. For each genotype, a total of 200 nuclei were analyzed.

[b] Depending on the strain, the thick structures appear to be fattened AEs or segments of tripartite SCs.

K348E defect in crossing over is correlated with spore viability, the *SPO13* gene was introduced into the NH246 series of diploids. These diploids were sporulated, and the resulting tetrads were dissected. As expected, the *red1*Δ *SPO13* diploid (NH246::pRS306 Spo13$^+$) produced 0.5% viable spores (49 asci), and the *RED1 SPO13* strain (NH246::pSB3 Spo13$^+$) generated 79.6% viable spores (76 asci). Only 13.8% of the spores from the *red1-K348E SPO13* diploid (NH246::pSB3-K348E Spo13$^+$; 76 asci) were viable. This value is statistically significantly lower than the 50% expected if spore viability is directly correlated with crossing over (χ^2; $P < 0.001$). These experiments suggest that the recombinants formed in the *red1-K348E* mutant, like those formed in the *red1*Δ mutant, are not productive for chromosome segregation (36).

The *red1-K348E* mutant fails to form mature SCs. It has been reported that *hop1* mutants can form extensive pieces of AEs (26), while *red1* mutants do not (36). To determine the cytological phenotype of a *red1-K348E* diploid, the SK1 *red1::LEU2* diploid YTS3 was transformed with vector pSB3 (*RED1*) or pSB3-K348E (*red1-K348E*), and chromosome spreads from sporulated diploids were examined by electron microscopy. Contrary to previously published results, thread-like structures were observed in some nuclei of the *red1::LEU2* strain (Table 6; Fig. 4). This difference may be due to the different strain background used in this work (SK1) compared to the BR strain background used by Rockmill and Roeder (36) and/or our fixation and spreading procedures. The observed structures may represent the AEs of unpaired chromosomes formed by Rec8p, a meiosis-specific cohesin protein that is required for Red1p localization to chromosomes (23). It is clear, however, that the cytological phenotype of *red1-K348E* is not equivalent to that of *red1::LEU2*. A statistically significant increase (χ^2, $P < 0.001$) in the number of cells with thicker threads is observed in *red1-K348E* compared to *red1::LEU2* (Table 6; Fig. 4). Some of these threads seem to be thickened AEs, but the majority are segments of tripartite SCs. Their branched appearance (Fig. 4D) suggests that they are connecting nonhomologous chromosomes. The segments of SC and thickened AEs are lacking in the isogenic *hop1* diploid, DW10. The SC fragments in *red1-K348E* may represent a leaky phenotype for the *red1-K348E* mutant in which local SC formation occurs

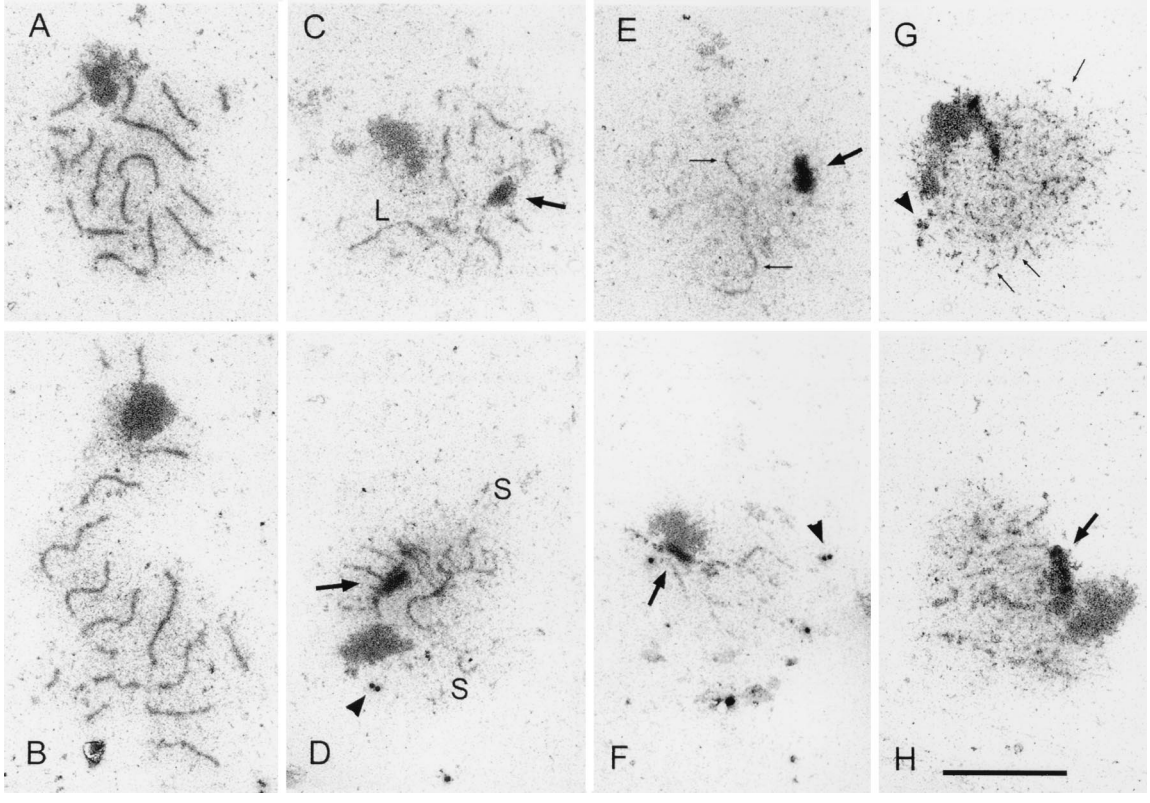

FIG. 4. SC formation in various wild-type and mutant SK1 strains. Chromosome spreads were prepared for electron microscopy as described in Materials and Methods. (A and B) YTS3::pSB3 (*RED1*); (C and D) YTS3::pSB3-K348E (*red1-K348E*); (E and F) YTS3::pRS306 (*red1::LEU2*); (G and H) DW10 (*hop1::LEU2*). The arrows point to polycomplexes, and the arrowheads point to unduplicated spindle pole bodies. The bar corresponds to 5 μm. S and L denote short and long regions of dense structures, respectively.

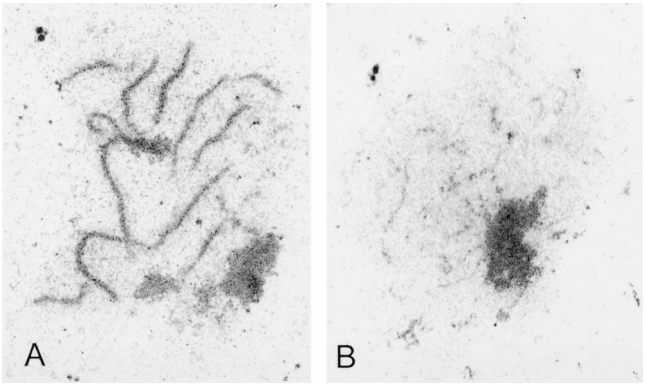

FIG. 5. SC formation in SK1 *red1* diploids overexpressing *HOP1*. Chromosome spreads were prepared for electron microscopy as described in Materials and Methods. (A) NH305::pBB14 (*red1-K348E*)/2μm *HOP1* (pNH83); (B) NH305::pRS402 (*red1::LEU2*)/2μm *HOP1* (pNH83).

because some Red1p-Hop1p hetero-oligomers are formed. Mature SCs were never observed in either *red1-K348E*, *red1::LEU2*, or *hop1* diploids (Table 6).

To test whether overexpression of *HOP1* can suppress the SC formation defect of *red1-K348E*, the SK1 diploids NH305::pRS402 (*red1::LEU2*) and NH305::pBB14 (*red1-K348E*) were transformed with pNH83 (2μm *HOP1*). Nuclei from meiotic cells were lysed, and chromosome spreads were examined by electron microscopy. Consistent with the observation that overexpression of *HOP1* failed to improve the spore viability of NH305::pRS402, there was no increase in the frequency of nuclei containing SC fragments in this strain (200 nuclei examined) (Fig. 5). While none of the nuclei from the *red1-K348E* diploid NH305::pBB14 formed wild-type SCs (Table 6), 10.5% of 200 nuclei from this strain exhibited nearly wild-type SCs when *HOP1* was overexpressed (Fig. 5). In addition, 23.5% of the nuclei from the *red1-K384E*/2μm *HOP1* diploid exhibited long fragments of SC, more than twice the number observed for the *red1-K348E* diploid without extra *HOP1* (Table 6). These results suggest that interaction of Red1p and Hop1p is essential for SC formation.

The meiotic progression and sporulation defects of *sae2*Δ/*com1*Δ are suppressed by null alleles of *RED1*, *HOP1*, and the *red1-K348E* mutant. Mutation of *RED1* can alleviate the meiotic arrests or delays caused by mutants that initiate recombination but then proceed aberrantly (49). This observation led to the hypothesis that *RED1* is part of a meiotic recombination checkpoint that monitors the progression of recombination and arrests the cell if the process goes awry (49). The *rad50S* mutant, for example, causes the formation of unprocessed DSBs which result in a delay in the meiotic divisions and a reduction in sporulation (1). *SAE2*/*COM1* is a gene which, when deleted, exhibits the same phenotypes as *rad50S*, including unprocessed DSBs, a delay in the onset of MI and MII, and a decrease in the number of mature asci (30, 35). To see whether the *sae2*Δ meiotic delay is dependent on *RED1* and *HOP1*, the kinetics of progression through MI and MII, as well as the ability to form mature asci, were compared in isogenic wild-type (NH305::pBB16), *sae2*Δ (NH306::pBB16), *red1::LEU2 sae2*Δ (NH306::pRS402), and *hop1::LEU2 sae2*Δ (NH311::pRS402) diploids.

Null alleles of both *RED1* and *HOP1* relieved the *sae2*Δ delay in the progression of the meiotic divisions, producing curves highly similar to the wild-type control curves (Fig. 6A). The number of cells able to complete MII was also improved by mutation of *HOP1* and *RED1*. Whereas the *sae2*Δ diploid produced only 21.7% tetranucleate cells by 10 h, 94.3 and 79.8% of the *red1::LEU2* and *hop1::LEU2* cells, respectively, were tetranucleate at the 10-h time point. In addition, *hop1::LEU2* and *red1::LEU2* partially suppressed the *sae2*Δ sporulation defect. The wild-type diploid produced 85.0% mature asci, compared to just 1.2% for the *sae2*Δ strain. In contrast, 34.7 and 41.2% mature asci were observed for the *red1::LEU2 sae2*Δ and *hop1::LEU2 sae2*Δ diploids, respectively.

The *sae2*Δ delay is triggered by the presence of unprocessed DSBs. In *rad50S* SK1 strains, deletion of *RED1* has no effect on DSBs (49), while *hop1* mutants exhibit approximately 10% the level of wild-type DSBs (cited in reference 49). To determine the effects of *hop1::LEU2* and *red1::LEU2* on DSBs in the *sae2*Δ SK1 diploids used for the time course analysis, the *THR4* DSB hot spot (48) was examined. The expected pattern of meiosis-specific DSBs was observed for *sae2*Δ, *red1::LEU2 sae2*Δ, and *hop1::LEU2 sae2*Δ (Fig. 7). Quantitation of the most prominent DSB fragment indicated that the *hop1::LEU2* and *red1::LEU2* diploids exhibited 11.9 and 46.8%, respectively, of the level of wild-type DSBs.

The *hop1* rescue of the *sae2*Δ delay could be due simply to the reduced number of DSBs relative to *red1*. In this case, the *red1-K348E sae2*Δ diploid should exhibit the same delays in meiotic progression and decreased sporulation observed for *sae2*Δ alone, since the number of DSBs observed in the *red1-K348E sae2*Δ strain is not greatly different from the number for the *RED1 sae2*Δ strain (66.5%) (Fig. 7). In contrast, if *HOP1* has a role in the checkpoint that involves interaction with *RED1*, the *red1-K348E* mutant should suppress the *sae2*Δ defects in meiotic progression and sporulation in a similar way as the *red1::LEU2* mutant. The latter result was observed. The *red1-K348E sae2*Δ diploid, NH306::pBB14, exhibited the same kinetics of progression through the meiotic divisions as the wild-type, *red1::LEU2 sae2*Δ, and *hop1::LEU2 sae2*Δ strains (Fig. 6A). Furthermore, the *red1-K348E sae2*Δ mutant produced increased levels of tetranucleate cells relative to the *sae2*Δ strain (82.7% versus 1.2%), as well more mature asci (20.2% versus 1.2%).

To see whether overexpression of *HOP1* can suppress the ability of *red1-K348E* to rescue the *sae2*Δ-induced delay in meiotic progression, *red1::LEU2* and *red1-K348E* diploids carrying either vector alone or a high-copy-number plasmid bearing *HOP1* (pDW72) were compared. Whereas overexpression of *HOP1* had no effect on the kinetics of meiotic progression in the *red1:LEU2* strain, the *red1-K348E* diploid overexpressing *HOP1* exhibited a greater delay in the onset of the meiotic divisions compared to *red1-K348E* containing vector alone (Fig. 6B).

DISCUSSION

HOP1 and *RED1* encode meiosis-specific proteins that are essential for the production of viable spores in yeast due to their roles in meiotic recombination and chromosome synapsis. Although no Red1p homologs have yet been identified in higher eukaryotes, the evolutionary conservation of Hop1p suggests that Red1p counterparts exist at the structural, if not the sequence, level. In fact, there are mammalian AE components (COR1 and SCP3) that may serve similar roles as Red1p (12, 24). Understanding how these two proteins function in yeast, therefore, is likely to provide insights into meiosis in metazoans as well.

Hop1p and Red1p both exhibit a variety of protein-protein interactions. In addition to forming hetero-oligomers with each other, each protein also exists as homo-oligomers (11, 20). Because *red1* and *hop1* mutants have overlapping as well

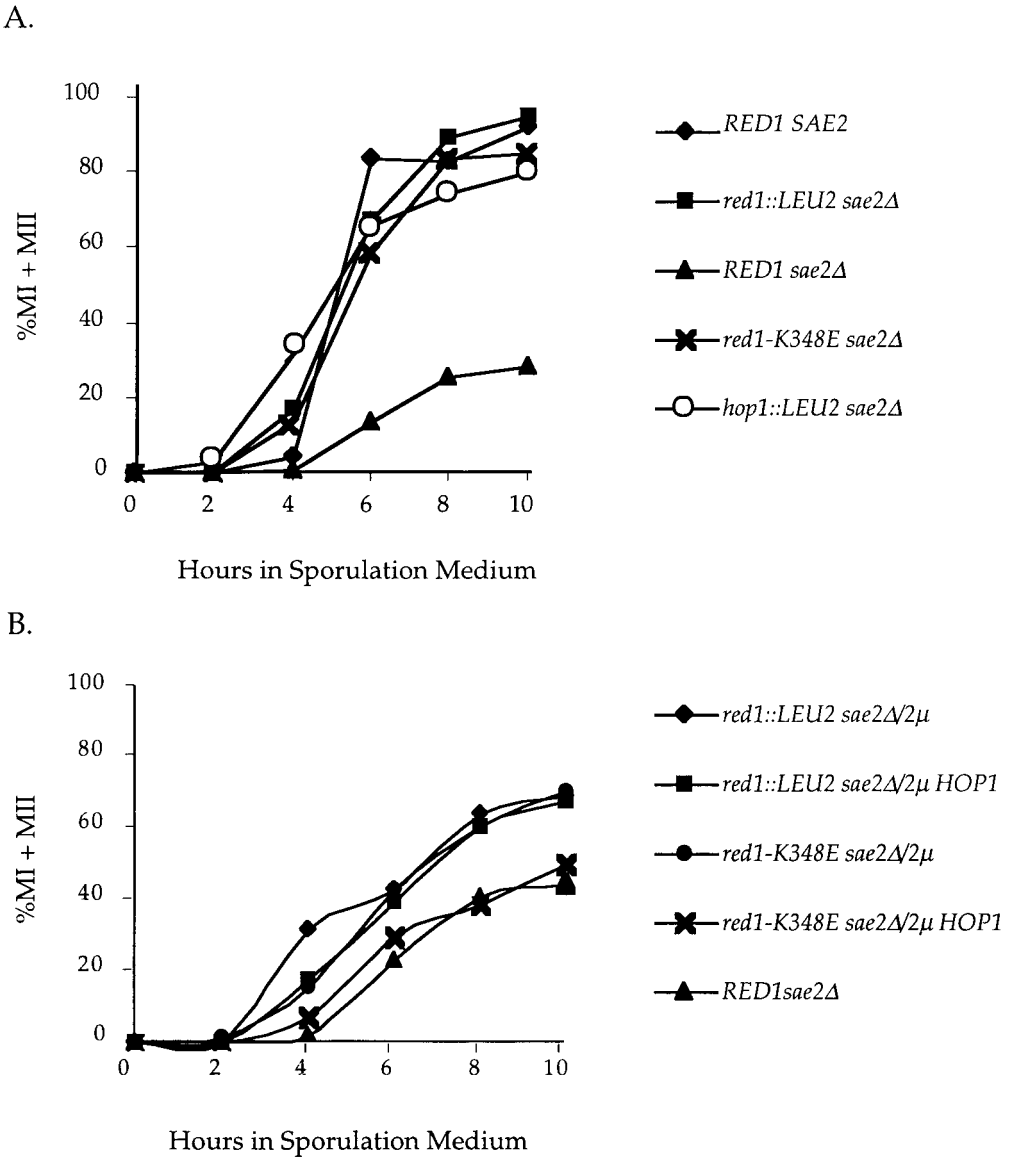

FIG. 6. Meiotic progression in various *red1 sae2*Δ SK1 diploids. Cells were fixed at different times after transfer to sporulation medium and stained with DAPI. The numbers of bi- and tetranucleate cells (indicative of passage through MI and MII, respectively) were determined by epifluorescence microscopy. Three independent cultures were examined for each strain. The graph shows the mean value for each diploid. (A) *RED SAE2*, NH305::pBB16; *red1::LEU2 sae2*Δ, NH306::pRS402; *RED1 sae2*Δ, NH306::pBB16; *red1-K348E sae2*Δ, NH306::pBB14; *hop1::LEU2 sae2*Δ, NH311::pRS402. (B) *red1::LEU2 sae2*Δ/2μm, NH306/pRS422; *red1::LEU2 sae2*Δ/2μm *HOP1*, NH306/pDW72; *red1-K348E sae2*Δ/2μm, NH306::pBB19/pRS422; *red1-K348E sae2*Δ/2μm *HOP1*, NH306::pBB19/pDW72; *RED1 sae2*Δ, NH306::pBB16.

as distinct phenotypes, it is clear that all three protein complexes (Hop1p-Hop1p, Red1p-Red1p, and Red1p-Hop1p) have roles during meiosis. The focus of this work is to define the functional requirements for Red1p-Hop1p hetero-oligomers by identifying separation-of-function mutants of *RED1* that specifically abolish interaction with Hop1p without affecting homo-oligomerization. Because deletion of a gene eliminates the protein from a cell, there can be pleiotropic effects if the protein serves more than one function. By specifically mutating the Hop1p interaction domain of Red1p, one can distinguish those processes that require hetero-oligomerization from those that do not.

The Hop1p interaction domain of Red1p was first defined by deletion analysis using the two-hybrid system. Two parts of Red1p were found to interact with Hop1p: a 30-amino-acid region between residues 330 and 359 and the last 291 amino acids of the protein. The finding that changing a single amino acid at position 348 in full-length Red1p is sufficient to disrupt Hop1p interaction suggests that the C terminus does not normally play an important role in complex formation with Hop1p. We propose that the interaction observed between *lexA-HOP1* and *GAD-RED1*$_{537–827}$ may result from a cryptic interaction site present in the C-terminal fragment that is not accessible in full-length Red1p when it is properly folded.

The sequence of a functional *RED1* homolog from a related yeast, *Kluyveromyces lactis*, has recently been published (42). The *K. lactis RED1* gene fully complements the spore inviability defect of an *S. cerevisiae red1* diploid even when present in low copy number. This result indicates that the *K. lactis* Red1 protein is able to interact efficiently with *S. cerevisiae* Hop1p and suggests that the Hop1p interaction domain of Red1p is conserved between the two yeasts. Although the *K. lactis* and

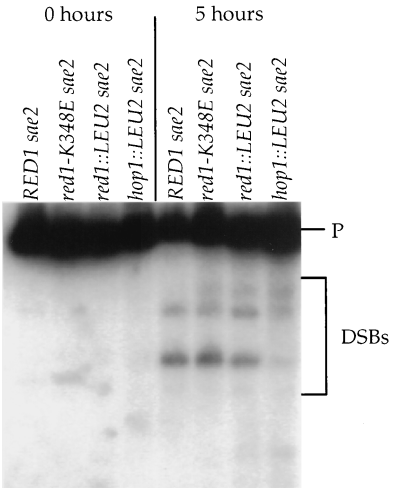

FIG. 7. DSBs analysis in SK1 diploids. DNA was isolated from vegetative cells (0 h) or cells 5 h after transfer to sporulation medium (5 h) as described in Materials and Methods. After digestion with *Bgl*II, the DNA was probed with a fragment to detect DSBs occurring near *THR4* (48). P represents the 10-kb parental fragment. The DSB fragments are indicated by the bracket. Strains used: NH306::pBB16 (*RED1 sae2*Δ); NH306::pBB14 (*red1-K384E sae2*Δ); NH306::pRS402 (*red1::LEU2 sae2*Δ); NH311::pRS402 (*hop1::LEU2 sae2*Δ).

S. cerevisiae proteins are only 26% identical over the entire length, there are small regions that exhibit stronger homology. In particular, there is a stretch of seven identical amino acids starting at position 347. The fact that the K-to-E mutation responsible for disrupting the Hop1p interaction maps to this stretch of amino acids supports the idea that this patch of the protein mediates binding of Hop1p to Red1p. The region of greatest homology between the two proteins resides in that last 93 amino acids, which are 59% identical (42). This region may represent the part of the C terminus that is required for Red1p homo-oligomerization.

How accurately one can interpret the mutant phenotypes of a separation-of-function allele depends on how confident one is that the only protein interaction affected is the one under consideration—in our case, Hop1p binding. Although we can not formally exclude the possibility that the *red1-K348E* point mutation also disrupts interaction with an unknown protein, there are a number of observations that support the idea that the sole defect in Red1-K348Ep is a reduced affinity for Hop1p. First, as noted above, the lysine at position 348 is within the 30-amino-acid Hop1p interaction domain defined independently by deletion analysis. Second, although few to no Red1-K348Ep-Hop1p complexes are detectable either by two-hybrid analysis or by co-IP experiments using meiotic extracts, wild-type levels of homo-oligomerization are observed for Red1-K348Ep. Third, the Red1-K348E protein is a stable phosphoprotein, indicating that its interactions with kinases such as Mek1p are not affected. Finally and most importantly, overexpression of *HOP1* allows suppression of the *red1-K348E* spore viability, SC formation, and meiotic checkpoint mutant phenotypes.

A likely function for Red1p-Hop1p complexes is in the formation of crossovers that are effective for MI segregation. It has been known for several years that the crossovers occurring in *red1* mutants are not functional for disjunction (36). This phenomenon could be explained by a failure in sister chromatid cohesion—a defect known to exist in *red1* diploids (4). Recently, however, we have shown genetically that *hop1* mutants also undergo crossovers that fail to ensure MI segregation (B. Baumgartner and N. M. Hollingsworth, unpublished data); yet *hop1* exhibits only a minimal defect in sister chromatid cohesion (4). Rather than propose two independent mechanisms for the generation of nonfunctional crossovers, we hypothesize that in order for recombination to generate a disjunction-competent crossover, the recombination intermediate must be formed in the presence of Red1p-Hop1p hetero-oligomers.

Analysis of interhomolog joint molecules (IHJMs) in *red1* mutants showed that *red1* specifically reduces IHJM but not intersister joint molecules (ISJMs) (40). *hop1* mutants have similarly been shown to reduce IHJMs while still allowing ISJMs to form (39). The decision whether joint molecules will be formed between sisters or homologs is made at the time of the DSB formation in *RED1* strains, and it is presumably this type of IHJM that is able to direct homolog disjunction. There are residual IHJMs in *red1* mutants (40). These IHJMs likely lead to crossovers that do not ensure MI segregation. It has been proposed that *RED1*-independent IHJMs arise from "rogue", or non-hot-spot-associated, DSBs (40). These authors noted that recombination around *TRP1* is *RED1* independent and that no DSB sites are detectable in the vicinity of *TRP1*.

Our model is that interaction between Hop1p and Red1p prior to or during DSB formation is what distinguishes a rogue DSB from one that can create a functional crossover. One idea is that hot-spot-associated DSBs are the ones that are used to make *RED1*-dependent functional crossovers. These DSBs occur in GC-rich domains (40). Hop1p has been demonstrated to have a strong preference for binding to GC-rich DNA (22, 32). Although the bulk of Hop1p requires Red1p to localize to chromosomes, we suggest that some Hop1p is bound near to DSBs independently of *RED1*. This idea is based on the observation that the levels of DSB are reduced in *red1 sae2*Δ diploids when *HOP1* is disrupted (N. M. Hollingsworth, unpublished data), indicating that *HOP1* is required for the formation and/or protection of DSBs even in the absence of *RED1*. In addition, *hop1* mutants have a more severe recombination defect than *red1* mutants (29, 36). DSBs occurring in GC-rich sequences may have a higher probability of having Hop1p nearby, which in turn can then associate with Red1p to form functional crossovers.

Analysis of crossing over in the *red1-K348E spo13* diploids supports the model that Red1p-Hop1p hetero-oligomers are required for the formation of crossovers effective for MI segregation. The *red1-K348E* mutant exhibited only a 2-fold reduction in crossing over compared, to an 11-fold reduction in the *red1*Δ mutant. This difference may be due to the fact that *RED1* is necessary for wild-type levels of DSBs in otherwise wild-type strains (29, 49). Perhaps the presence of the Red1-K348Ep allows for the protection of DSBs from aberrant processing, and therefore there are more ends available for the generation of recombination intermediates compared to the *red1*Δ. Despite just a twofold reduction in recombination, however, the *red1-K348E SPO13* diploid exhibited low levels of spore viability (13.8%). This low spore viability is not because there is a threshold of recombination which must be reached that is higher than a twofold reduction allows, since a number of mutants are known to decrease recombination two- to threefold and reduce spore viability only to 50 to 60% (e.g., *zip1*, *zip2*, *msh4* and *msh5*) (10, 21, 38, 44). More likely is the idea that the crossovers occurring in *red1-K348E*, like the crossovers in *red1*Δ and *hop1*Δ diploids, are unable to direct proper homolog segregation at the first meiotic division.

hop1 mutants make pieces of AEs but fail to undergo synapsis (18, 26). This defect in SC formation could be due to the reduced number of DSBs in *hop1* strains or because the re-

combination intermediates that are generated in the absence of Red1p-Hop1p hetero-oligomers are unable to allow synapsis (or both). Given that *red1-K348E sae2*Δ diploids produce nearly wild-type levels of DSBs, it seems unlikely that a limiting number of breaks is the problem. Furthermore, overexpression of *HOP1* specifically in the presence of *red1-K348E* results in some nuclei with nearly wild-type levels of SC. This result provides strong evidence that a lack of Red1p-Hop1p hetero-oligomers is responsible for the SC formation defect. The improvement in the spore viability of *red1-K348E* diploids when *HOP1* is overexpressed is presumably due to the ability to now form SCs. It may be that the stable connections required for synapsis are the same recombination intermediates that are processed to make functional crossovers.

Red1p is a phosphoprotein whose phosphorylation is dependent on the meiosis-specific kinase, Mek1p (4, 11). *RED1* and *MEK1* are required for a checkpoint that monitors meiotic recombination and arrests or delays meiosis if recombination is proceeding improperly (49). Red1p and Mek1p have been proposed to provide a chromosomal context in which recombination intermediates must be generated if they are to be sensed by the checkpoint (49). Recently it was demonstrated that Red1p is phosphorylated by Mek1p in response to the initiation of recombination by the formation of DSBs (3). Dephosphorylation of Red1p by the Glc7p phosphatase is then necessary for cells to exit pachytene in the BR strain background (3). The dephosphorylation of Red1p presumably occurs when recombination intermediates have been properly resolved. Our work indicates that Redlp-Hoplp hetero-oligomers are necessary for the recombination checkpoint to function in the SK1 strain background. We propose that recombination intermediates must be processed in the presence of Red1p-Hop1p complexes for the recombination checkpoint to be triggered. It seems likely that the requirement of Red1p-Hop1p hetero-oligomers for generating SCs and segregation-competent crossovers is mechanistically linked to their role in the meiotic recombination checkpoint.

ACKNOWLEDGMENTS

We thank Neta Dean, JoAnne Engebrecht, Bernadette Holdener, Michael Lichten, and Aaron Neiman for helpful discussions. JoAnne Engebrecht and Aaron Neiman gave useful comments on the manuscript. Julie Bailis, JoAnne Engebrecht, Stan Hollenberg, Michael Lichten, and Rolf Sternglanz generously supplied plasmids and/or strains.

This work was supported by two grants to N.M.H.: NIH grant GM50717 and a grant from the Pew Charitable Trusts. J.L. was supported by the Austrian Science Fund (grant S 8202).

REFERENCES

1. **Alani, E., R. Padmore, and N. Kleckner.** 1990. Analysis of wildtype and *rad50* mutants of yeast suggests an intimate relationship between meiotic chromosome synapsis and recombination. Cell **61:**419–436.
2. **Bai, C., and S. J. Elledge.** 1997. Gene identification using the yeast two-hybrid system. Methods Enzymol. **283:**141–156.
3. **Bailis, J. M., and G. S. Roeder.** 2000. Pachytene exit controlled by reversal of Mek1-dependent phosphorylation. Cell **101:**211–221.
4. **Bailis, J. M., and G. S. Roeder.** 1998. Synaptonemal complex morphogenesis and sister-chromatid cohesion require Mek1-dependent phosphorylation of a meiotic chromosomal protein. Genes Dev. **12:**3551–3563.
5. **Bascom-Slack, C. A., L. O. Ross, and D. S. Dawson.** 1997. Chiasmata, crossovers and meiotic chromosome segregation. Adv. Genet. **35:**253–284.
6. **Borde, V., T. C. Wu, and M. Lichten.** 1999. Use of a recombination reporter insert to define meiotic recombination domains on chromosome III of *Saccharomyces cerevisiae*. Mol. Cell. Biol. **19:**4832–4842.
7. **Brachmann, C. B., A. Davies, G. J. Cost, E. Caputo, J. Li, P. Hieter, and J. D. Boeke.** 1998. Designer deletion strains derived from *Saccharomyces cerevisiae* S288C: a useful set of strains and plasmids for PCR-mediated gene disruption and other applications. Yeast **14:**115–132.
8. **Campbell, D. A., S. Fogel, and K. Lusnak.** 1975. Mitotic chromosome loss in a disomic haploid of *Saccharomyces cerevisiae*. Genetics **79:**383–396.
9. **Caryl, A. P., S. J. Armstrong, G. H. Jones, and F. C. H. Franklin.** 2000. A homologue of the yeast *HOP1* gene is inactivated in the Arabidopsis meiotic mutant *asy1*. Chromosoma **109:**62–71.
10. **Chua, P. R., and G. S. Roeder.** 1998. Zip2, a meiosis-specific protein required for the initiation of chromosome synapsis. Cell **93:**349–359.
11. **de los Santos, T., and N. M. Hollingsworth.** 1999. Red1p: a *MEK1*-dependent phosphoprotein that physically interacts with Hop1p during meiosis in yeast. J. Biol. Chem. **274:**1783–1790.
12. **Dobson, M. J., R. E. Pearlman, A. Karaiskakis, B. Spryopoulos, and P. B. Moens.** 1994. Synaptonemal complex proteins: occurrence, epitope mapping and chromosome disjunction. J. Cell Sci. **107:**2749–2760.
13. **Engebrecht, J., J. Hirsch, and G. S. Roeder.** 1990. Meiotic gene conversion and crossing over: their relationship to each other and to chromosome synapsis and segregation. Cell **62:**927–937.
14. **Goutte, C., and A. D. Johnson.** 1988. a1 protein alters the DNA binding specificity of the α2 repressor. Cell **52:**875–882.
15. **Heyting, C.** 1996. Synaptonemal complexes: structure and function. Curr. Opin. Cell Biol. **8:**389–396.
16. **Hollenberg, S. M., R. Sternglanz, P. F. Cheng, and H. Weintraub.** 1995. Identification of a new family of tissue-specific basic helix-loop-helix proteins with a two-hybrid system. Mol. Cell. Biol. **15:**3813–3822.
17. **Hollingsworth, N. M., and B. Byers.** 1989. *HOP1*: a yeast meiotic pairing gene. Genetics **121:**445–462.
18. **Hollingsworth, N. M., L. Goetsch, and B. Byers.** 1990. The *HOP1* gene encodes a meiosis-specific component of yeast chromosomes. Cell **61:**73–84.
19. **Hollingsworth, N. M., and A. D. Johnson.** 1993. A conditional allele of the *Saccharomyces cerevisiae HOP1* gene is suppressed by overexpression of two other meiosis-specific genes: *RED1* and *REC104*. Genetics **133:**785–797.
20. **Hollingsworth, N. M., and L. Ponte.** 1997. Genetic interactions between *HOP1*, *RED1* and *MEK1* suggest that *MEK1* regulates assembly of axial element components during meiosis in the yeast, *Saccharomyces cerevisiae*. Genetics **147:**33–42.
21. **Hollingsworth, N. M., L. Ponte, and C. Halsey.** 1995. *MSH5*, a novel MutS homolog, facilitates meiotic reciprocal recombination between homologs in *Saccharomyces cerevisiae* but not mismatch repair. Genes Dev. **9:**1728–1739.
22. **Kironmai, K. M., K. Muniyappa, D. B. Friedman, N. M. Hollingsworth, and B. Byers.** 1998. DNA-binding properties of Hop1 protein, a synaptonemal complex component from *Saccharomyces cerevisiae*. Mol. Cell. Biol. **18:**1424–1435.
23. **Klein, F., P. Mahr, M. Galova, S. B. C. Buonomo, C. Michaelis, K. Nairz, and K. Nasmyth.** 1999. A central role for cohesins in sister chromatid cohesion, formation of axial elements and recombination during meiosis. Cell **98:**91–103.
24. **Lammers, J. H. M., H. H. Offenberg, M. van Aalderen, A. C. G. Vink, A. J. J. Dietrich, and C. Heyting.** 1994. The gene encoding a major component of the lateral elements of synaptonemal complexes of the rat is related to X-linked lymphocyte-regulated genes. Mol. Cell. Biol. **14:**1137–1146.
25. **Loidl, J., F. Klein, and J. Engebrecht.** 1998. Genetic and morphological approaches for the analysis of meiotic chromosomes in yeast. Methods Cell Biol. **53:**257–285.
26. **Loidl, J., F. Klein, and H. Scherthan.** 1994. Homologous pairing is reduced but not abolished in asynaptic mutants of yeast. J. Cell Biol. **125:**1191–1200.
27. **Malone, R. E., and R. E. Esposito.** 1981. Recombinationless meiosis in *Saccharomyces cerevisiae*. Mol. Cell. Biol. **1:**891–901.
28. **Maniatis, T., E. F. Fritsch, and J. Sambrook.** 1982. Molecular cloning: a laboratory manual. Cold Spring Harbor Laboratory, Cold Spring Harbor, N.Y.
29. **Mao-Draayer, Y., A. M. Galbraith, D. L. Pittman, M. Cool, and R. E. Malone.** 1996. Analysis of meiotic recombination pathways in the yeast *Saccharomyces cerevisiae*. Genetics **144:**71–86.
30. **McKee, A. H. Z., and N. Kleckner.** 1997. A general method for identifying recessive diploid-specific mutations in *Saccharomyces cerevisiae*, its application to the isolation of mutants blocked at intermediate stages of meiotic prophase and characterization of a new gene *SAE2*. Genetics **146:**797–816.
31. **Muhlrad, D., R. Hunter, and R. Parker.** 1992. A rapid method for localized mutagenesis of yeast genes. Yeast **8:**79–82.
32. **Muniyappa, K., S. Anuradha, and B. Byers.** 2000. Yeast meiosis-specific protein Hop1 binds to G4 DNA and promotes its formation. Mol. Cell. Biol. **20:**1361–1369.
33. **Nag, D. K., H. Scherthan, B. Rockmill, J. Bhargava, and G. S. Roeder.** 1995. Heteroduplex DNA formation and homolog pairing in yeast meiotic mutants. Genetics **141:**75–86.
34. **Parent, S. A., C. M. Fenimore, and K. A. Bostian.** 1985. Vector systems for studying DNA sequences. Yeast **1:**83–138.
35. **Prinz, S., A. Amon, and F. Klein.** 1997. Isolation of *COM1*, a new gene required to complete meiotic double-strand induced recombination in *Saccharomyces cerevisiae*. Genetics **146:**781–795.
36. **Rockmill, B., and G. S. Roeder.** 1990. Meiosis in asynaptic yeast. Genetics **126:**563–574.
37. **Rockmill, B., and G. S. Roeder.** 1988. *RED1*: a yeast gene required for the

segregation of chromosomes during the reductional division of meiosis. Proc. Natl. Acad. Sci. USA **85:**6057–6061.
38. **Ross-Macdonald, P., and G. S. Roeder.** 1994. Mutation of a meiosis-specific MutS homolog decreases crossing over but not mismatch correction. Cell **79:** 1069–1080.
39. **Schwacha, A., and N. Kleckner.** 1994. Identification of joint molecules that form frequently between homologs but rarely between sister chromatids. Cell **76:**51–63.
40. **Schwacha, A., and N. Kleckner.** 1997. Interhomolog bias during meiotic recombination: meiotic functions promote a highly differentiated interhomolog-only pathway. Cell **90:**1123–1135.
41. **Sikorski, R. S., and P. Hieter.** 1989. A system of shuttle vectors and yeast host strains designed for efficient manipulation of DNA in *Saccharomyces cerevisiae*. Genetics **122:**19–27.
42. **Smith, A. V., and G. S. Roeder.** 2000. Cloning and characterization of the *Kluyveromyces lactis* homologs of the *Saccharomyces cerevisiae RED1* and *HOP1* genes. Chromosoma **109:**50–61.
43. **Smith, A. V., and G. S. Roeder.** 1997. The yeast Red1 protein localizes to the cores of meiotic chromosomes. J. Cell Biol. **136:**957–967.
44. **Sym, M., and G. S. Roeder.** 1994. Crossover interference is abolished in the absence of a synaptonemal complex protein. Cell **79:**283–292.
45. **Thompson, D. A., and F. W. Stahl.** 1999. Genetic control of recombination partner preference in yeast meiosis. Isolation and characterization of mutants elevated for meiotic unequal sister-chromatid recombination. Genetics **153:**621–641.
46. **Tu, J., W. Song, and M. Carlson.** 1996. Protein phosphatase type I interacts with proteins required for meiosis and other cellular processes in *Saccharomyces cerevisiae*. Mol. Cell. Biol. **16:**4199–4206.
47. **Vershon, A. K., N. M. Hollingsworth, and A. D. Johnson.** 1992. Meiotic induction of the yeast *HOP1* gene is controlled by positive and negative regulatory elements. Mol. Cell. Biol. **12:**3706–3714.
48. **Wu, T.-C., and M. Lichten.** 1994. Meiosis-induced double-strand break sites determined by yeast chromatin structure. Science **263:**515–518.
49. **Xu, L., B. M. Weiner, and N. Kleckner.** 1997. Meiotic cells monitor the status of the interhomolog recombination complex. Genes Dev. **11:**106–118.
50. **Zetka, M. C., I. Kawasaki, S. Strome, and F. Muller.** 1999. Synapsis and chiasma formation in *Caenorhabditis elegans* require *HIM-3*, a meiotic chromosome core component that functions in chromosome segregation. Genes Dev. **13:**2258–2270.